Hybrid Type Reinforcement of Highway Embankment against Earthquake Induced Damage

Hemanta Hazarika[1], Chengjiong Qin[1], Yoshifumi Kochi[2], Hideo Furuichi[3], Nanase Ogawa[4] and Masanori Murai[5]

[1] Kyushu University, Fukuoka 819-0395, Japan
[2] K's Lab Inc., Yamaguchi 753-0212, Japan
[3]Adachi Architectural Design Office Co., Ltd., Tokyo 141-0031, Japan
[4]Giken Ltd., Tokyo 135-0063, Japan
[5]Shimizu Corporation, Tokyo 104-8370, Japan
Hazarika@civil.kyushu-u.ac.jp

Abstract. In this research, a hybrid type pile system is proposed as a countermeasure of embankment failures during earthquakes. In the proposed technique, inclined piles are added in addition to the rows of vertical steel pipe piles. Inclined piles are expected to reduce ground deformation and settlement due to earthquakes, especially when the embankment widths are large. The focus of the research is to evaluate the stability of embankments by the external force of the earthquake and to elucidate the mechanism of the reinforcement effect by the vertical steel pipe piles and inclined piles. Model tests using shaking table and their numerical simulations were performed to evaluate the performance of the hybrid type reinforcement measures. Model tests were conducted by taking into the consideration the pile rigidity and embedment depth. The numerical simulations were also performed in which the effect of the inclination of the inclined piles was also taken into the consideration. Both the test results and numerical simulations have confirmed that in embankment with hybrid reinforcement measures, the increase in excess pore water pressure during an earthquake could be suppressed, and the settlement of the embankment could be significantly reduced.

Keywords: Shaking table tests, Dynamic effective stress analysis, Embankment settlement, Highway embankment, Hybrid retrofitting technique, Liquefaction

1 Introduction

In the recent earthquakes in Japan, many geotechnical structures, such as river dykes, levees, dams, and road embankments, suffered extensive damage and failures [1–2]. Highway embankments are strategic infrastructures that play a critical role in connecting and transporting vital rescue components and disaster relief supplies after natural disasters such as earthquakes, tsunami, typhoons, and rainstorms occur. Many highway embankments in Japan are aging as they were constructed more than six decades ago,

and therefore, the Ministry of Land, Infrastructure, Transport, and Tourism (MLIT, Japan) is very much concerned about the vulnerabilities of those during natural disasters. Fig. 1 shows an example of liquefaction-induced ground deformation of a highway embankment during the 2016 Kumamoto Earthquake [3]. Few case studies on the seismic failure of the structures and the influence of the liquefiable foundation soil during the recent earthquakes are described in [4–6]. It is of utmost importance to mitigate seismically induced damage to road embankments, and therefore, it is essential to develop sustainable and economic ground improvement techniques that are in line with the current policy of the Japanese government.

Piles are often used to mitigate earthquake-induced damage to embankments. When piles are subjected to intense dynamic loads during earthquakes, soil-structure interaction plays an essential role in the response of piles [7]. Recent observations after major earthquakes have shown that substantial damage and destruction can still be encountered in pile foundations. The behavior of piles in liquefiable soil layers is much more complex than that of the non-liquefiable soil layer due to the decreasing stiffness and shear strength of the surrounding soil due to the increase in pore water pressure during earthquakes. [8-9]. Many researchers have conducted shaking table tests on the dynamic behavior of pile foundations in liquefiable soils [10-14]. Also, it could be confirmed that restraining the pile heads from rotating increases the maximum shear strength and the piles act as a monolithic structure leading to uniform deformation of piles [15]. Previous studies on beam-pile and anchor-pile supported embankments using shaking table tests have shown that the anchor-pile systems can better support the embankment slopes than that of beam-piles [16]. The purpose of this research is to develop an appropriate deformation countermeasures to protect the existing highway embankments and remediate the associate ground settlements during earthquakes.

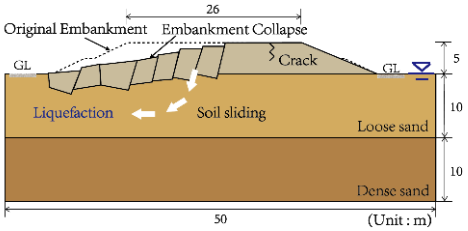

Fig. 1. Failure of road embankment during the 2016 Kumamoto earthquake [3]

A hybrid type pile system is proposed as a countermeasure of embankment failures during earthquakes, as shown in Fig. 2. In this proposed technique, inclined piles are added in addition to the rows of vertical steel pipe piles, as shown in the figure. Inclined piles are expected to reduce ground deformation and settlement, especially when the embankment widths are large. The focus of the research was to evaluate the stability of embankments by the external force of the earthquake and to elucidate the mechanism of the reinforcement effect by the steel pipe piles and inclined piles. Model tests using shaking table and their numerical simulations were performed to evaluate the performance of the reinforcement measures quantitatively. An embankment model with reinforcement measures was created, and a series of shaking table tests were conducted by

taking into the consideration the pile rigidity and embedment depth. The numerical simulations were performed using dynamic effective stress analysis.

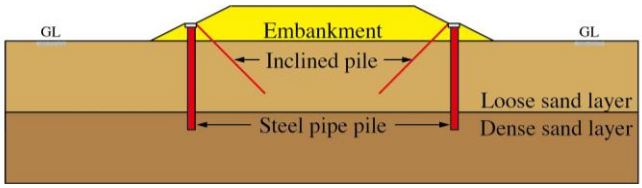

Fig. 2. Proposed countermeasure [17]

2 Shaking Table Tests

In this study, a series of shaking table tests were conducted to confirm the effectiveness of the proposed seismic retrofitting of road embankment. The test series also investigated the effect of repeated load in the form of foreshock and mainshock, such as those observed during the 2016 Kumamoto earthquake. The performances of the unreinforced embankment, existing reinforcement measures, and proposed measures were evaluated.

2.1 Test Conditions

In shaking table tests, a box-shaped soil box with height 800 mm, width 1800 mm, and depth 400 mm was used. The box was made of a transparent acrylic plate, and, therefore, the behavior of the ground during earthquake loadings could be observed. Toyoura sand was used as soil for both embankment and foundation soil. The relative density of the embankment was set to 60%, and the foundation soil was prepared by dividing it into a loose upper layer (relative density 60%) and a lower layer (relative density 90%). The scale ratio was set to 50, and the parameters for the ground, steel pipe pile, and inclined pile were determined as shown in Table 1 using the scaling law [18]. Aluminum pipes were used as vertical piles using the similarity ratio in Table 1. The inclined piles were made of steel. The locations of each measuring device (accelerometer, water pressure gauge, displacement gauge) are shown in the Fig. 3.

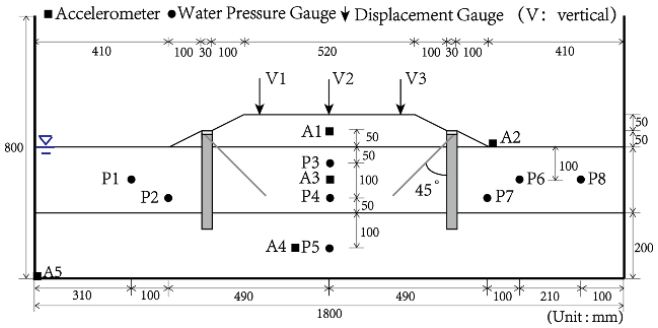

Fig. 3. Instrumentations for the shaking table tests

Table 1. Similitude for 1g shaking table tests

Parameter	Prototype/model	Scaling factor
Length	N	50
Density	1	1
Stress	N	50
Pore water pressure	N	50
Acceleration	1	1
Displacement	$N^{1.5}$	353.55
Permeability	$N^{0.75}$	18.80
Axial stiffness of piles	$N^{2.5}$	17,677
Bending stiffness of piles	$N^{3.5}$	883,883
Friction	1	1

Layouts of the four different cases, which were used in the tests, are shown in Fig. 4. Case 1 is an embankment without reinforcement, and Case 2 is a case of existing countermeasure work using only vertical steel pipe piles. Case 3 is a case where geogrid was used for Case 2. Case 4 is a hybrid-type reinforced embankment case using both vertical pile and inclined pile. The vertical pile and the inclined pile were fixed in their heads. The tip of each vertical pile was inserted up to the dense soil layer with a relative density of 90%. In Case 3 and Case 4, to prevent soil movement between the piles, geogrid was used to connect the piles as shown in Figs. 4(c) and 4(d).

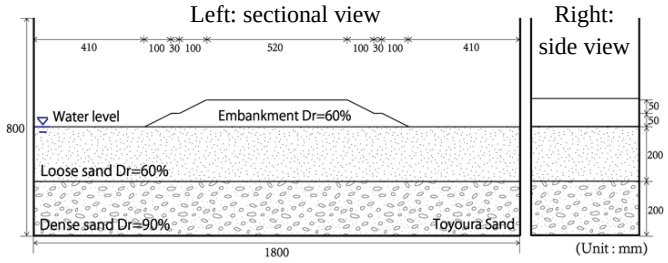

(a) Case 1 - unreinforced foundation of the embankment

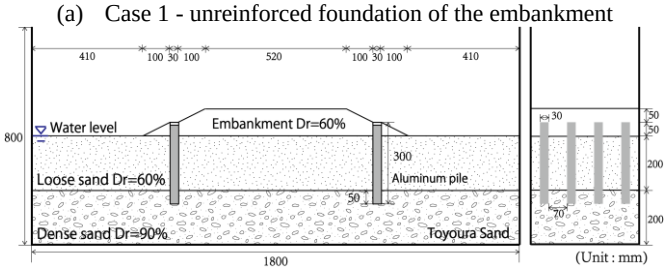

(b) Case 2 - only two rows of vertical piles reinforcement

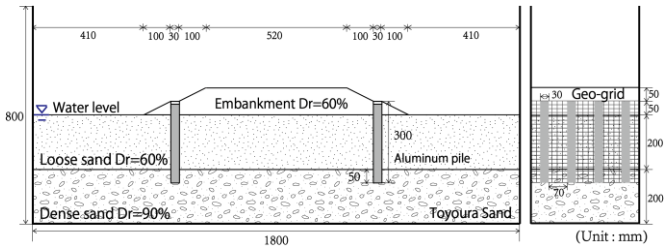

(c) Case 3 - two rows of combined geo-grid and vertical piles reinforcement

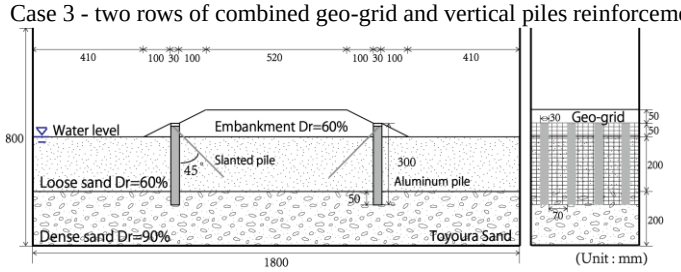

(d) Case 4 - hybrid type reinforcement

Fig. 4. Layouts of models (left: sectional view and right: side view): (a) Case 1 - unreinforced foundation of the embankment, (b) Case 2 - only two rows of vertical piles reinforcement (c) Case 3 - two rows of combined geo-grid and vertical piles reinforcement and (d) Case 4 - hybrid vertical piles and inclined piles system reinforcement

The locations of the measuring devices (excess pore water pressure gauges, accelerometers, displacement gauges) are shown in Fig. 4. Dynamic loadings were imparted sequencially in the form of foreshock (=200 Gal), mainshock (=300 Gal), and strong motion (=400 Gal). The frequency of dynamic loadings was determined according to scaling laws and recorded acceleration data at the KMMH16 station during the 2016 Kumamoto earthquake. Tests were conducted using a sine wave with a frequency of 10 Hz and dynamic time of 10 s.

2.2 Results and Discussions

Excess Pore Water Pressure Ratio ($R_u = \Delta u/\sigma'_v$)

Figs. 5 and 6 show the excess pore water pressure ratios at two locations (P3 and P4 in Fig. 4) just below the center of the embankment due to two dynamic loadings (foreshock = 200 Gal and mainshock = 300 Gal). From these figures, it can be seen that in the case of the unreinforced embankment, the pore water pressure ratio reaches 1.0 in both the foreshock and the mainshock, and the foundation soil is completely liquefied. However, in Case 3 and Case 4, the increase in pore water pressure is minimal in both the foreshock and the mainshock, and therefore, it can be said that these measures could effectively prevent liquefaction. Especially in Case 3, there is a delay in the development of excess pore water pressure. For the proposed measures (Case 4), no increase of the excess pore water pressures could be observed.

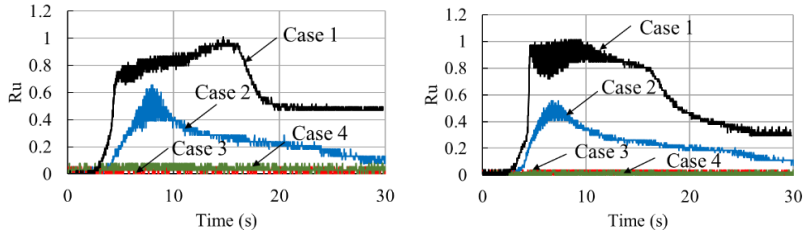

(a) Ru measured at P3 (b) Ru measured at P4

Fig. 5. Time histories of excess pore water pressure ratio during foreshock: (a) Ru measured at P3 and (b) Ru measured at P4

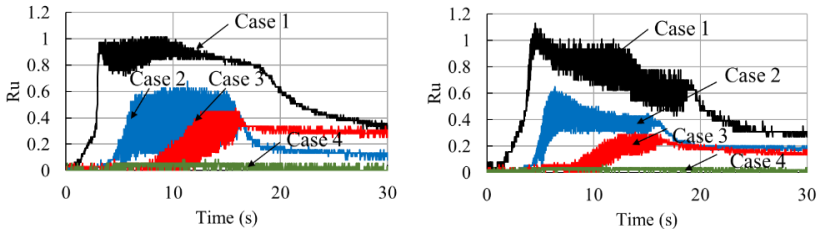

(a) Ru measured at P3 (b) Ru measured at P4

Fig. 6. Time histories of excess pore water pressure ratio during the mainshock: (a) Ru measured at P3 and (b) Ru measured at P4

Fig. 7 shows the maximum pore water pressure ratio (Ru) at different depths measured by each water pressure gauge. From Fig. 7, it could be clarified that, in the case of the unreinforced embankment, the value of the pore water pressure ratio exceeded 1.0 in both 200 Gal and 300 Gal in the shallow part, leading to the liquefaction of the foundation soil. On the other hand, in the case of the reinforced embankment (Case 2, Case 3, Case 4), the increase in pore water pressure is suppressed in 200 Gal (Ru <0.7). In Case 3 and Case 4, although a slight increase of Ru was seen at the mainshock (Ru was 0.5 or less), no liquefaction occured. From these results, it can be said that the developed countermeasure is the most effective in preventing liquefaction of the foundation soil in both the foreshock (200 Gal) and the mainshock (300 Gal).

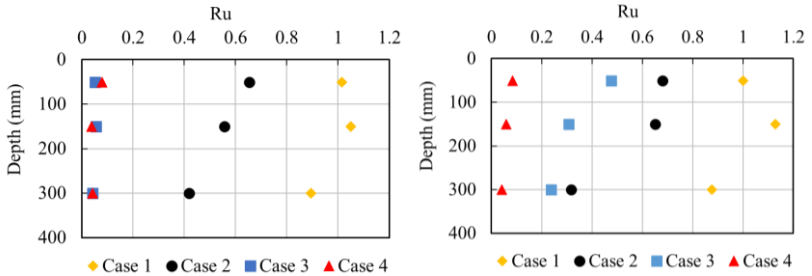

(a) The peak of Ru during the foreshock (b) The peak of Ru during the mainshock

Fig. 7. The peak of excess pore water pressure ratio during the foreshock and mainshock: P3 (50mm below ground), P4 (150mm below ground), and P5 (300mm below ground)

Settlement of Embankment

Figs. 8 and 9 show the time history of the settlement of three locations (V1, V2, and V3) on the embankment during the dynamic loadings (foreshock = 200 Gal, mainshock = 300 Gal) measured by three displacement gauges. In the case of the foreshock (Fig. 8), both Case 1 and Case 2 show an increasing trend in the settlement. However, in the case of the mainshock (Fig. 9), all the other cases except for the hybrid type reinforcement measure (Case 4) show a rising trend. In the case of the unreinforced embankment, significant settlement (24 cm on the model scale; 1.2 m on the prototype) occurs during the mainshock. However, the settlements in the case of the reinforced embankments drastically reduced. In particular, in the case of the hybrid type reinforcement, it could be seen that there is almost no settlement in both the foreshock and the mainshock. One particular observation worthy of noting here is that with increasing reinforcing measures (vertical pile, geogrid reinforced vertical pile and hybrid type reinforcement), there is a delay in the occurrence of settlement.

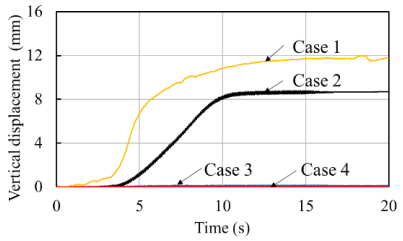

(a) Vertical displacement measured at V1

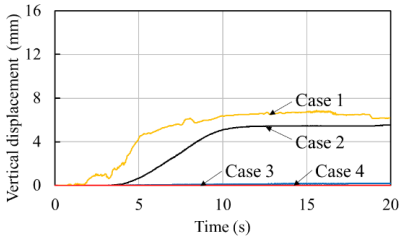

(b) Vertical displacement measured at V2

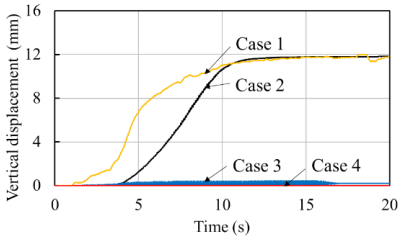

(c) Vertical displacement measured at V3

Fig. 8. Time histories of vertical displacement during the foreshock: (a) the left crest – V1, (b) the middle – V2, and (c) the right crest – V3

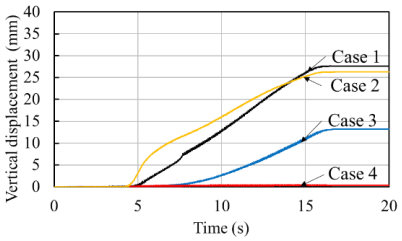

(a) Vertical displacement measured at V1

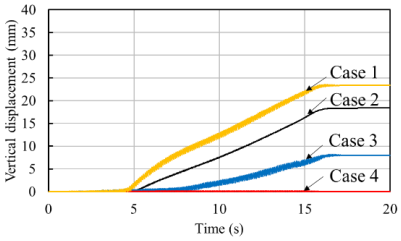

(b) Vertical displacement measured at V2

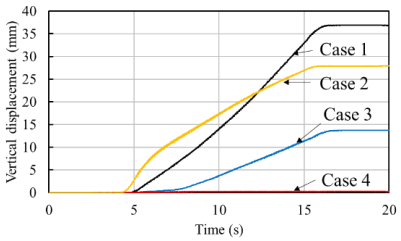

(c) Vertical displacement measured at V3

Fig. 9. Time histories of vertical displacement during the mainshock: (a) the left crest – V1, (b) the middle – V2, and (c) the right crest – V3

Figs 10 and 11 show the seismic resistance of embankments at different dynamic loadings (foreshocks, mainshocks, and strong earthquakes), which were manually measured at the end of each loading. From Fig. 10, it could be confirmed that in the embankment with no reinforcement (Case 1), a large settlement (30 mm) occurs even during foreshock (Fig. 10b). Fig. 11a displays that a large deformation in the embankment took place after the mainshock, making further test beyond that impossible. From Fig. 11, it could be seen that embankment without inclined piles (Case 3) shows less settlement (11.6 mm) than the unreinforced embankment (37 mm) during the mainshock. In contrast, embankment with both vertical piles and inclined piles, barely experiences settlement in both the foreshock and the mainshock. In addition, the embankment using hybrid type reinforcement shows less settlement (12.6 mm) than the embankment reinforced by only vertical piles (36.5 mm) experiencing motion stronger than main shock (Fig. 11b).

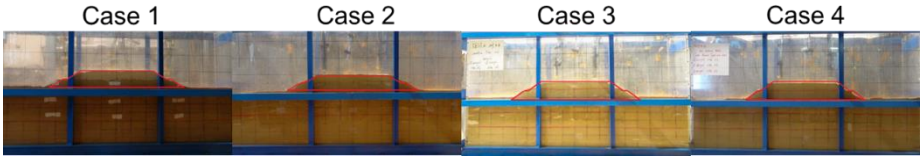

(a) Before dynamic loadings

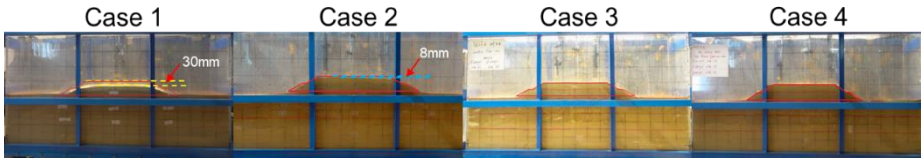

(b) After the foreshock

Fig. 10. Performance comparison during the foreshock in each case

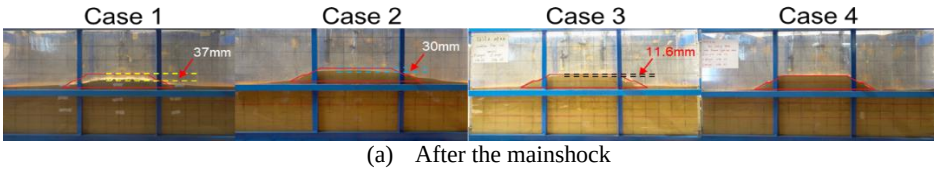

(a) After the mainshock

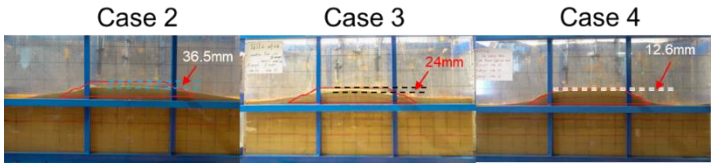

(b) After the strong motion

Fig. 11. Performance comparison during the mainshock and strong motion in each case

Deformation of Pile Heads

Fig. 12 shows the top view of of the test model showing the heads of the piles. Residual deformations of the tips of the piles were measured at the end of each loading for all the cases are plotted in Figs. 13 and 14. From these results, it can be seen that in the case of the hybrid type reinforcement measures (Case 4), the amount of horizontal deformation is the smallest for both the foreshock (200 Gal) and the mainshock (300 Gal).

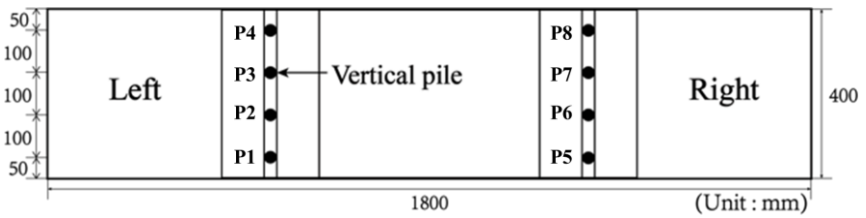

Fig. 12. Top view of the test model

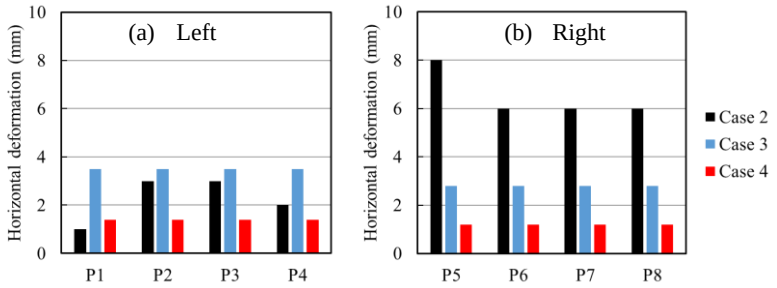

Fig. 13. Residual deformation of pile heads on the left (a) and right (b) during the foreshock

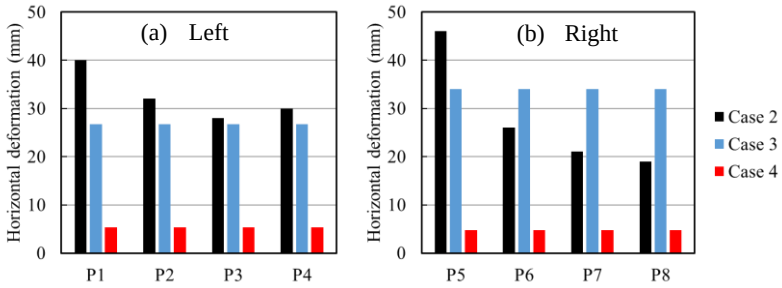

Fig. 14. Residual deformation of pile heads on the left (a) and right (b) during the mainshock

3 Numerical Analysis

The shaking table tests could confirm that the new countermeasure method developed in this research has the effect of suppressing the deformation of the embankment during earthquake. However, in order to elucidate the mechanism, numerical simulations using dynamic effective stress analysis were carried out to reproduce the dynamic behaviors of each case.

3.1 Simulation Models

Fig. 15 shows all the analysis models (Case 1, Case 2, Case 3, and Case 4). The embankment and ground conditions are the same as those in the shaking table tests. Case 4 is the condition, in which the inclination angle of the inclined pile was set to 60 °, to investigate the effect of installation conditions on the reinforcing effect. The lateral and bottom boundaries in the numerical models were fixed to imitate the boundary conditions of the test models. The lateral and bottom boundaries are assumed to be impermeable, whereas the surface of the loose sand layer is a permeable boundary. In order to ensure numerical stability, the time integration increment was selected to be 0.001s. Fig. 16 shows the input acceleration (mainshock), measured on the shaking table. In this analysis, this waveform was used as the input motion, which was imparted to the model's bottom.

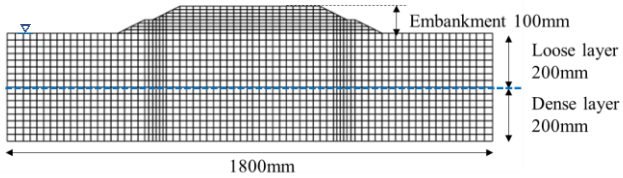

(a) Case 1 - unreinforced foundation of the embankment

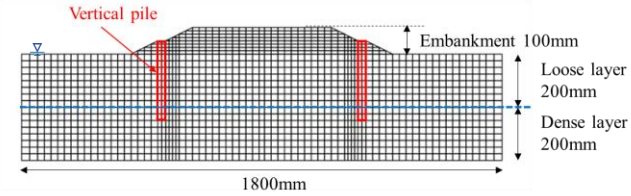

(b) Case 2 - only two rows of vertical piles reinforcement

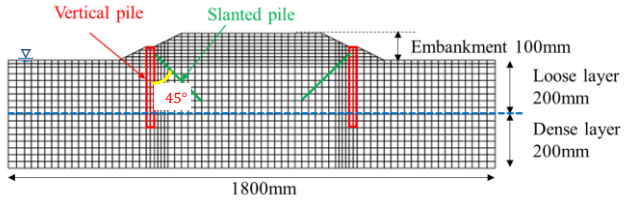

(c) Case 3 - hybrid type reinforcement ($\theta = 45°$)

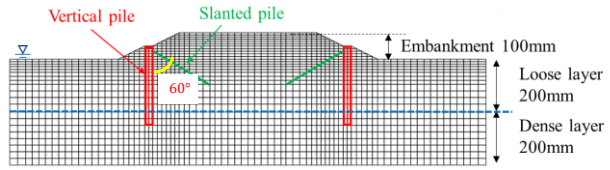

(d) Case 4 - hybrid type reinforcement ($\theta = 60°$)

Fig. 15. Layouts of models: (a) Case 1 - unreinforced foundation of the embankment, (b) Case 2 - only two rows of vertical piles reinforcement (c) Case 3 - hybrid type reinforcement ($\theta = 45°$) and (d) Case 4 - hybrid type reinforcement ($\theta = 60°$)

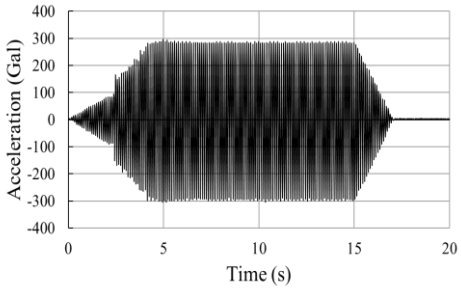

Fig. 16. Input motion

3.2 Materials Parameters

Table 2 shows the parameters used for the dynamic effective stress analysis. Cyclic elasto-plastic model was selected as the constitutive law for the soils in the embankment and foundation. Table 3 shows the material characteristics of the vertical and inclined piles. The inclined piles were modeled as beam elements. For vertical pile, hybrid beam element, consisting of the conventional beam element and elastic solid element, was used to represent the pile volume [19]. The joint elements were introduced along all the interfaces between the soil and piles, which share identical displacements in the horizontal direction.

Table 2. Material parameters of the constitutive model

Material parameters		Loose sand layer Dr = 60%	Dense sand layer Dr = 90%	Embankment
Density	ρ	1.88	2.00	1.88
Coefficient of permeability	k	0.01	0.01	0.01
Initial void ratio	e_0	0.738	0.659	0.738
Compression index	λ	0.02	0.0004	0.02
Swelling index	κ	0.0005	0.00008	0.0005
Failure stress ratio	M_f^*	1.300	1.466	1.300
Phase transformation stress ratio	M_m^*	0.980	0.765	0.980
Initial shear modulus ratio	G_0/σ_m^*	2343	1133	2343
Dilatancy parameters	D_0^*	0.5	0.12	0.5
	n	5.0	4.0	5.0
Hardening parameters	B_0^*	6550	54000	6550
	B_1^*	65.5	5400	65.5
Reference strain parameter	γ_r^{P*}	0.002	0.03	0.002
	γ_r^{E*}	0.008	0.36	0.008

Table 3. Material parameters of the constitutive model (reinforcing material)

Parameters	Unit	Vertical pile	Inclined pile
Young's modulus	MN/m^2	73000	206000
Bending stiffness	MN· m^2	3.43×10^{-3}	8.2×10^{-7}

3.3 Simulation Results

Excess Pore Water Pressure Ratio (R_u = Δu/σ'$_v$)

Figs. 17 and 18 show the distribution of excess pore water pressure ratio at the end of foreshock and mainshock. As evident from these figures, in the case of unreinforced embankments and the reinforcement using only vertical piles, the excess pore water pressure ratio reaches 1.0 in both the foreshock and the mainshock, and the foundation soil is completely liquefied. However, in Case 3 and Case 4, the increase in pore water pressure is sufficiently suppressed during the foreshock (200 Gal), where the Ru value

is less than 0.3. In the mainshock (300 Gal), Case 4 shows the rise of Ru in some parts of the embankment, however, that could not lead to complete liquefaction. Case 3, with 45 degree inclination of the inclined piles, did not experience any significant rise in the Ru value even during mainshock. Based on these results, it can be said that the developed countermeasure is very effective in preventing liquefaction of the foundation soil during earthquake.

Fig. 19 shows the excess pore water pressure ratio observed at location at P4 (refer to Fig. 4) due to the mainshock. The figure reveals that, in Case 1 and Case 2, the excess pore water pressure ratio rises immediately, and after reaching the peak, it takes sufficient time for the excess pore water pressure to dissipate. However, in Case 4, the increase of Ru was delayed and got dissipiated immediately after the dynamic loading stopped. On the other hand, in Case 3, the increase in excess pore water pressure was relatively small, and it gradually disappeared. Therefore, it can be said that the combination of vertical pile and inclined pile, and the inclination angle play an important role in preventing shear deformation of soils and, therefore, liquefaction. The deformations behaviors of the embankment are discussed in the following sub-section.

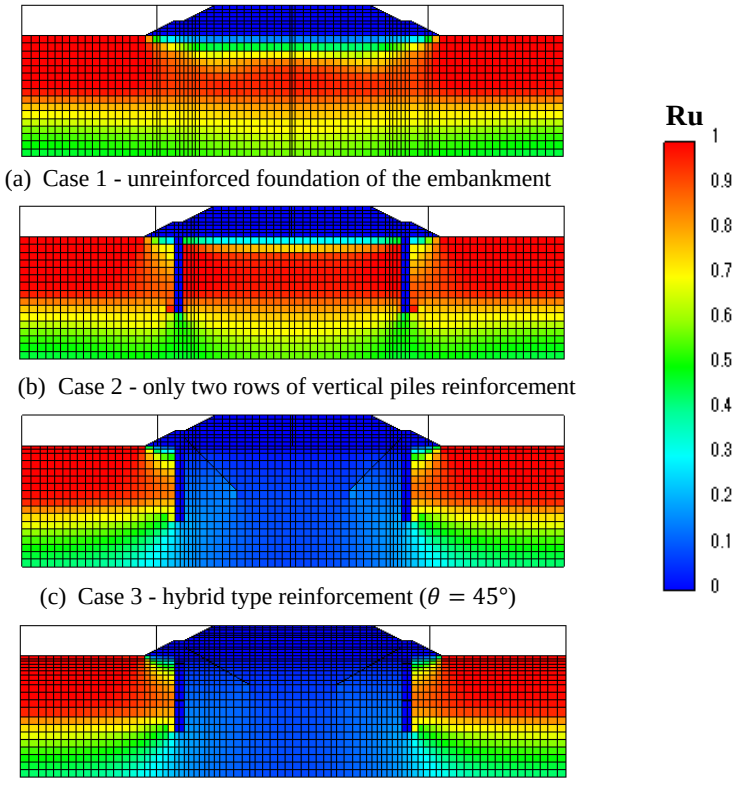

(a) Case 1 - unreinforced foundation of the embankment

(b) Case 2 - only two rows of vertical piles reinforcement

(c) Case 3 - hybrid type reinforcement ($\theta = 45°$)

(d) Case 4 - hybrid type reinforcement ($\theta = 60°$)

Fig. 17. Distribution of excess pore water pressure ratio at the end of the foreshock

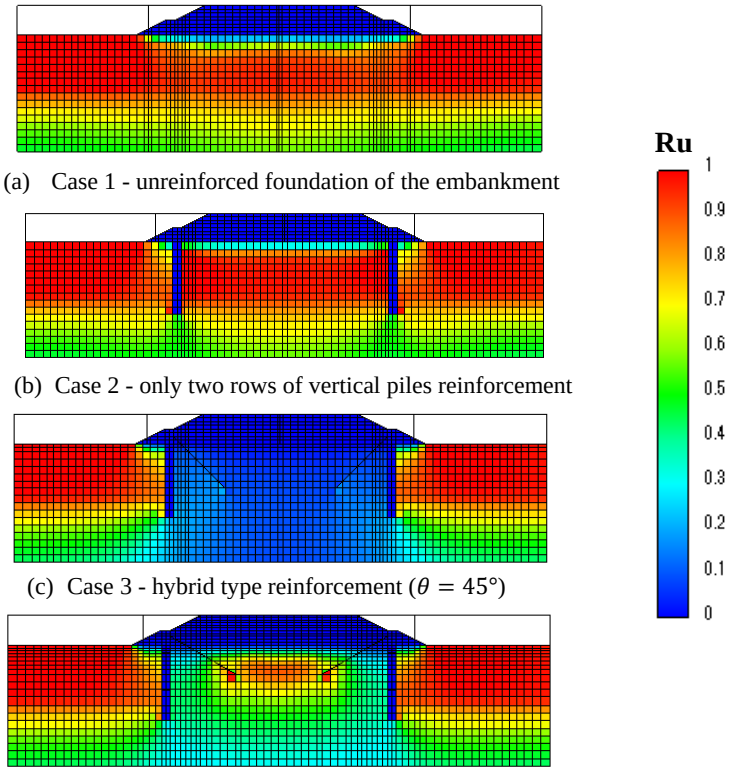

(a) Case 1 - unreinforced foundation of the embankment

(b) Case 2 - only two rows of vertical piles reinforcement

(c) Case 3 - hybrid type reinforcement ($\theta = 45°$)

(d) Case 4 - hybrid type reinforcement ($\theta = 60°$)

Fig. 18. Distribution of excess pore water pressure ratio at the end of the mainshock

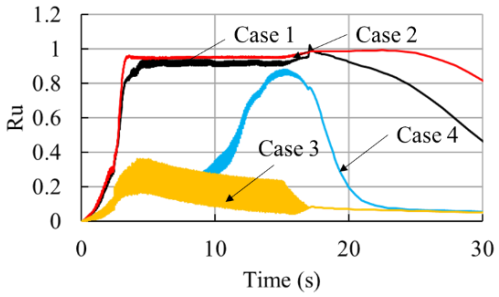

Fig. 19. Time history of excess pore water pressure ratio (P3)

Deformation of Embankment and Foundation Soils

Figs. 20 and 21 show the deformed configuration of the four cases at the end of the foreshock and the mainshock. In the case of the unreinforced embankment (Case 1) as well as embankment only with vertical piles (Case 2), large deformation occurs during the mainshock, leading to large embankment settlement. However, in Case 3 and Case

4, deformation of the foundation soil is suppressed, and as a result, embankment settlement could be reduced. In Case 3 (inclination angle = 45 °), there is no significant settlement in both the foreshock and the mainshock. In Case 4 (inclination angle = 60 °), however, the deformations of the foundation soil and the embankmengt are found to be larger during the mainshock.

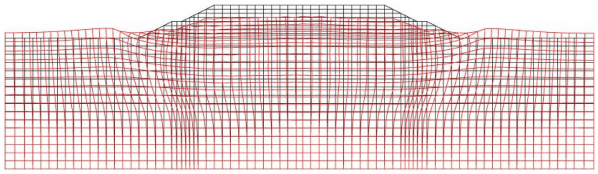

(a) Case 1 - unreinforced foundation of the embankment

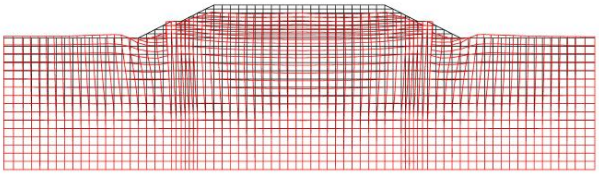

(b) Case 2 - only two rows of vertical piles reinforcement

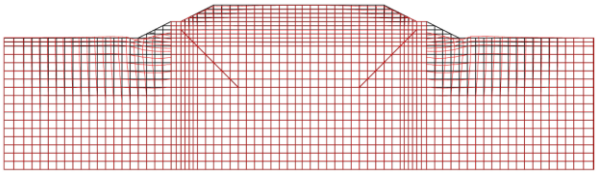

(c) Case 3 - hybrid type reinforcement ($\theta = 45°$)

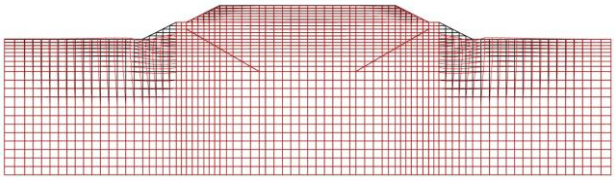

(d) Case 4 - hybrid type reinforcement ($\theta = 60°$)

Fig. 20. Deformed configuration at the end of the foreshock (Blackline: Before shaking; Red line: After shaking)

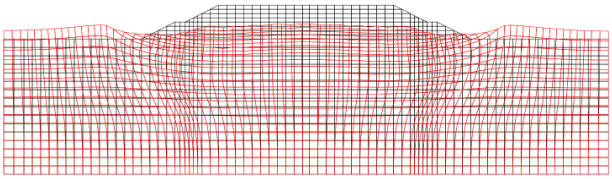

(a) Case 1 - unreinforced foundation of the embankment

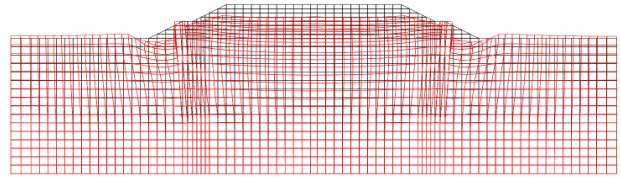

(b) Case 2 - only two rows of vertical piles reinforcement

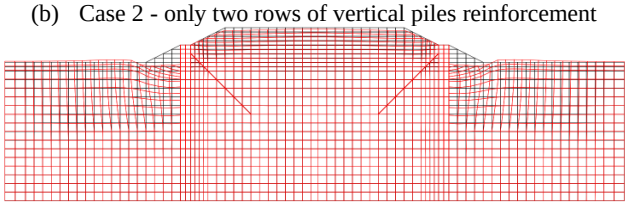

(c) Case 3 - hybrid type reinforcement ($\theta = 45°$)

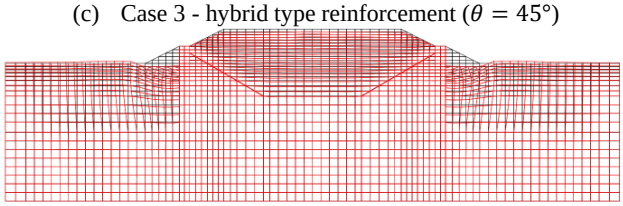

(d) Case 4 - hybrid type reinforcement ($\theta = 60°$)

Fig. 21. Deformed configuration at the end of the foreshock (Blackline: Before shaking; Red line: After shaking)

Fig. 22 shows the time history of settlements in the central part of the embankment, (similar to V2 in the shaking table model), due to the mainshock for all the four cases. In Case 1 and Case 2, the settlement progresses linearly immediately after the dynamic loading. However, the hybrid type reinforcements (Case 3 and Case 4) show a considerable delay in the occurrence of settlement, and the final settlements were only 1/5 to 1/7 to those of Case 1 and Case 2. These results once again prove that the installation angle of inclined piles has significant contribution towards preventing the settlement of embankment.

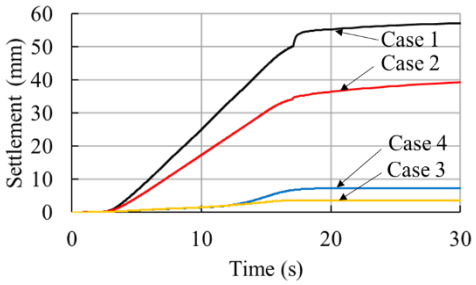

Fig. 22. Time history of the settlement (V2)

4 Comparison of Test and Simulation Results

The results for Case 1 (unreinforced embankment) and Case 3 (hybrid type reinforcement $\theta = 45°$) are selected as typical results for comparisons. The comparisons between analysis (denoted "Ana.") and test (denoted "Tes.") results divulge the predictive capacity of the simulation. The computed results were found to be in good agreement with that observed in the tests, including the settlement and the development of excess pore pressures ratio.

4.1 Excess Pore Water Pressure Ratio (Ru)

The excess pore water pressure ratios (Ru) at the three locations (P3, P4, and P5) directly under the embankment for unreinforced embankment (Case 1), are shown in Fig. 23 and Fig. 24 for the forshock and mainshock respectively. It can be seen that the analysis results and the test results are showing almost the same trend. At P3 and P4, both the analysis and test results show that the loose sand layer liquefied completely. However, no liquefaction is observed in the dense soil layer, as confirmed from the values of Ru (< 0.8) at P5. It is to be noted that the trends of the dissipation phase in the analysis are slightly different from those in the tests. This may be due to some limitations of the constitute models used in the analysis.

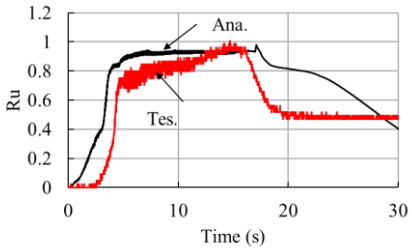

(a) P3

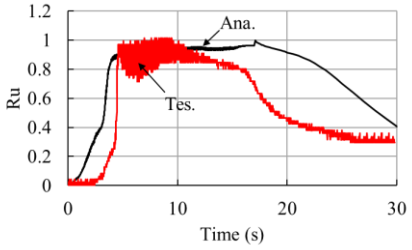

(b) P4

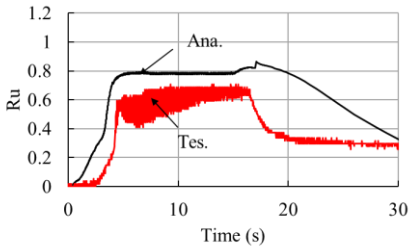

(c) P5

Fig. 23. Computed and measured time histories of excess pore water pressure ratio in Case 1 during the foreshock (a) P3, (b) P4, and (c) P5

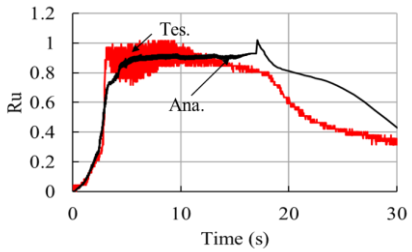

(a) P3

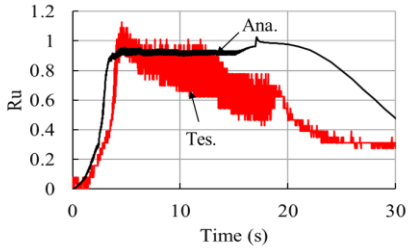

(b) P4

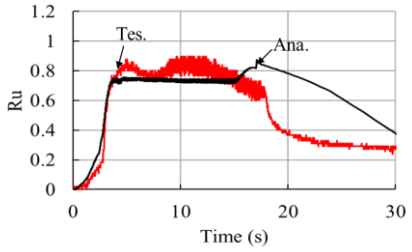

(c) P5

Fig. 24. Computed and measured time histories of excess pore water pressure ratio in Case 3 during the mainshock (a) P3, (b) P4, and (c) P5

Results similar to those in Figs. 23 and 24 are shown in Figs 25 and 26 for the hybrid type reinforcement (Case 3). These figures reveal that, in comparison with unreinforced foundations, hybrid type reinforcement can limit the development of excess pore water pressure effectively. The Ru values reaches only up to 0.2 to 0.3, and dissipation starts very quickly, confirming the liquefaction prevention capacity of the proposed measure. However, for both the foreshock and mainshock, the analysis results deviate from the test results. This particular aspects needs to be explored further in the future.

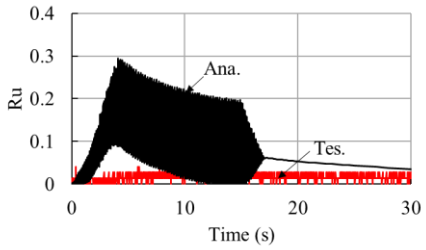

(a) P3

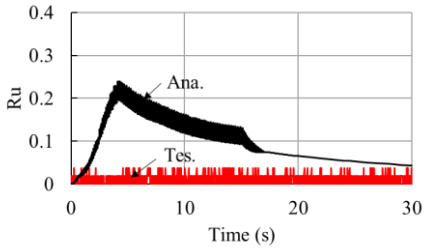

(b) P4

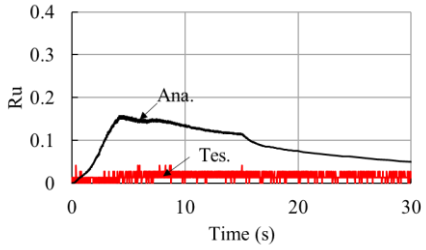

(c) P5

Fig. 25. Computed and measured time histories of excess pore water pressure ratio in Case 3 during the foreshock (a) P3, (b) P4, and (c) P5

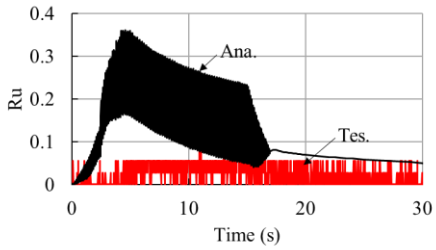

(a) P3

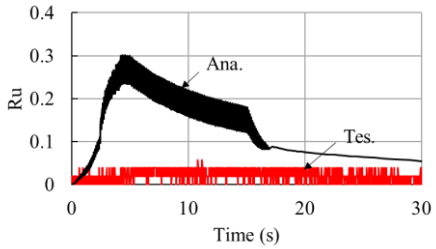

(b) P4

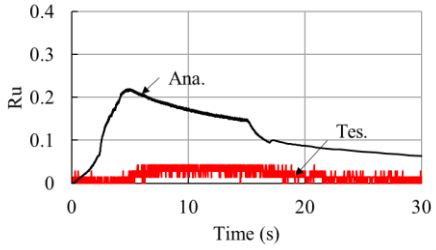

(c) P5

Fig. 26. Computed and measured time histories of excess pore water pressure ratio in Case 3 during the mainshock (a) P3, (b) P4, and (c) P5

4.2 Embankment Settlement

The numerical results are selected at the same locations (V1, V2 and V3) of the shaking table test models (Refer to Fig. 3). Figs. 27 and 28 show the comparison between the numerical and test results for the settlement of embankment in the unreinforced case (Case 1) due to the dynamic loading. The time histories of numerical results during both foreshock and mainshock show qualitative agreement with the test results. The computed settlements in the middle of the embankment (V2), however, are larger than the test results.

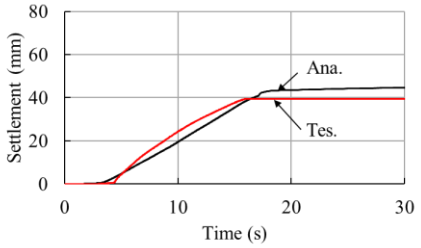

(a) V1

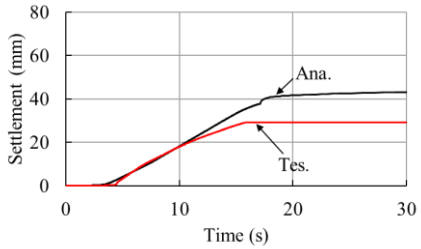

(b) V2

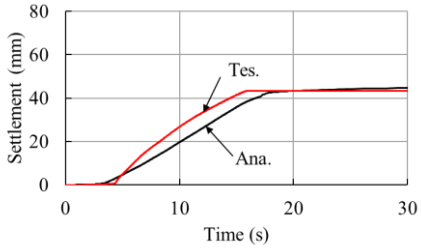

(c) V3

Fig. 27. Computed and measured time histories of settlement in Case 1 during the foreshock (a) V1, (b) V2, and (c) V3

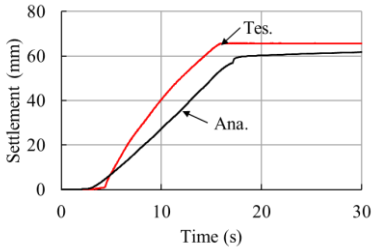

(a) V1

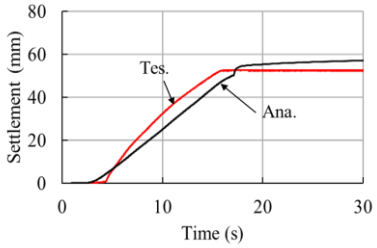

(b) V2

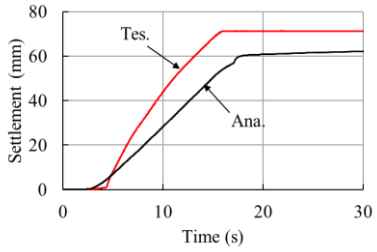

(c) V3

Fig. 28. Computed and measured time histories of settlement in Case 1 during the mainshock (a) V1, (b) V2, and (c) V3

Figs. 29 and 30 show the comparison between the numerical and test results of the embankment settlement for hybrid type reinforcement (Case 3). For both the foreshock and the mainshock, the numerical results are much higher than the test results, and this point needs to be re-examined in the future.

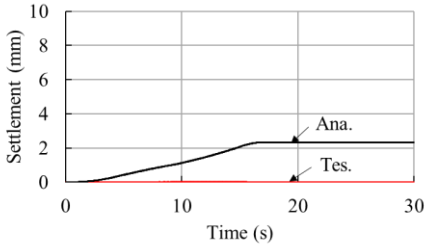

(a) V1

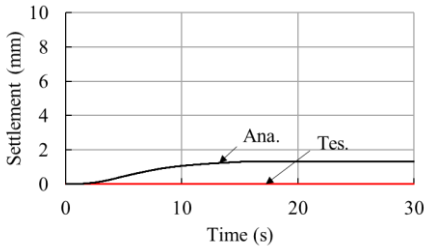

(b) V2

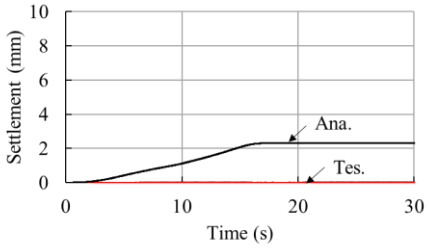

(c) V3

Fig. 29. Computed and measured time histories of settlement in Case 3 during the foreshock (a) V1, (b) V2, and (c) V3

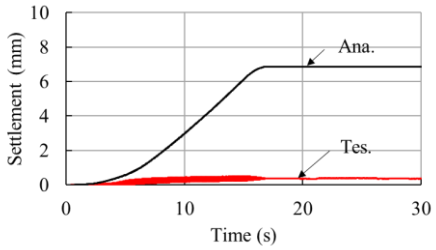

(a) V1

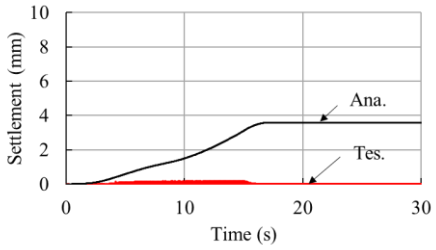

(b) V2

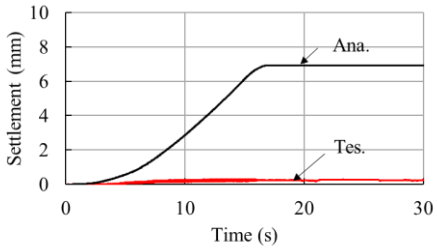

(c) V3

Fig. 30. Computed and measured time histories of settlement in Case 3 during the mainshock (a) V1, (b) V2, and (c) V3

5 Conclusions

In this study, we proposed a hybrid type seismic retrofitting work for road embankment using vertical pile and inclined pile and examined its effectiveness by using shaking table tests and numerical analysis. The main conclusions are described below.

1. The main causes of embankment settlement during an earthquake are large deformation of the foundation soil and resulting liquefaction. Large settlement and horizontal displacement occur even in the foreshock in the case of embankment where no countermeasures against earthquake is adopted.
2. In the embankment with hybrid type reinforcement measures, the increase in excess pore water pressure during an earthquake could be suppressed due to limited shear deformation of the foundation soils, and the settlement of the embankment could be significantly reduced.
3. In hybrid type reinforcement, it is more effective to install the inclined piles at an angle of 45 °. It is, however, necessary to further investigate the effect of the inclination and length of inclined piles.
4. The seismic performance of the proposed countermeasure is superior to the reinforcement measures for embankments using only vertical steel pipe piles.

6 Acknowledgment

A major part of this research was supported by the research grant from Nippon Expressway Company Limited (NEXCO) and affiliated organizations, Japan. Also, a part of this research was funded by Kyushu Regional Management Service Association, Fukuoka, Japan. The authors gratefully acknowledge those financial supports. The authors also would like to thank Mr. Daisuke Matsumoto of Japan Foundation Eng., Co., Ltd., Mr. Takashi Fujishiro of Geo-Disaster Prevention Institute, Mr. Shinichiro Ishibashi of Nihon Chiken Co., Ltd., Dr. Naoto Watanabe of KFC Ltd. and Mr. Shigeo Yamamoto of Chuo Kaihatsu Corporation for their support in this research. Last but not least, the authors are indebted to Mr. Yuichi Yahiro, technical staff of Department of Civil Engineering, Kyushu University, for his continuous advice and cooperation during the shaking table tests.

References

1. Sasaki, Y., Towhata, I., Miyamoto, K., Shirato, M., Narita, A., Sasaki, T. and Sako, S.: Reconnaissance report on damage in and around river levees caused by the 2011 off the Pacific coast of Tohoku Earthquake. Soils and Foundation 52(5), 1016–32 (2012).
2. Hazarika, H., Kokusho, T., Kayen, R.E., Dashti, S., Fukuoka, H., Ishizawa, T., Kochi, Y., Matsumoto, D., Furuichi, H., Hirose, T., Fujishiro, T., Okamoto, K., Tajiri, M. and Fukuda, M.: Geotechnical damage due to the 2016 Kumamoto earthquake and future challenges, Lowland Technology International 19(3), 189-204 (2017).
3. West Nippon Expressway Company Limited: Kumamoto Earthquake Response Committee WG2 Report: About earthquake resistance performance of highway embankment (2017).

4. Maharjan, M. and Takahashi, A.: Liquefaction-induced deformation of earthen embankments on non-homogeneous soil deposits under sequential ground motions. Soil Dynamics and Earthquake Engineering 66, 113-124 (2014).
5. Ishikawa, H., Saito, K., Nakagawa, K. and Uzuoka, R.: Liquefaction analysis of a damaged river levee during the 2011 Tohoku earthquake. In: Computer methods and recent advances in geomechanics: proceedings of the 14th international conference of international association for computer methods and recent advances in geomechanics, 673–677, Taylor & Francis, Kyoto (2014).
6. Oka, F., Tsai, P., Kimoto, S. and Kato, R.: Damage patterns of river embankments due to the 2011 off the Pacific Coast of Tohoku Earthquake and a numerical modeling of the deformation of river embankments with a clayey subsoil layer. Soils and Foundations 52(5), 890-909 (2012).
7. Mylonakis G. and Gazetas G.: Seismic soil-structure interaction: beneficial or detrimental, Journal of Earthquake Engineering 4(3):277-301 (2000).
8. Lu, C.W., Oka, F. and Zhang, F.: Analysis of soil–pile–structure interaction in a two-layer ground during earthquakes considering liquefaction. International Journal for Numerical and Analytical Methods in Geomechanics 32(8), 863-895 (2008).
9. Rahmani, A. and Pak, A.: Dynamic behavior of pile foundations under cyclic loading in liquefiable soils, Computers and Geotechnics 40, 114–126(2012).
10. Abdoun, T. and Dobry, R.: Evaluation of pile foundation response to lateral spreading, Soil Dynamics and Earthquake Engineering 22(9), 1051–1058 (2002).
11. Bhattacharya, S., Madabhushi, S. P. G. and Bolton, M. D.: An alternative mechanism of pile failure in liquefiable deposits during earthquakes. Geotechnique 54(3) 203-213 (2004).
12. Yao, S., Kobayashi, K., Yoshida, N. and Matsuo, H.: Interactive behavior of soil–pile-superstructure system in transient state to liquefaction by means of large shake table tests. Soil Dynamics and Earthquake Engineering 24(5), 397-409 (2004).
13. Suzuki, H., Tokimatsu, K., Sato, M. and Abe, A.: Factor affecting horizontal subgrade reaction of piles during soil liquefaction and lateral spreading. In Seismic performance and simulation of pile foundations in liquefied and laterally spreading ground, 1-10, ASCE, (2006).
14. Dungca, J.R., Kuwano, J., Takahashi, A., Saruwatari, T., Izawa, J., Suzuki, H. and Tokimatsu, K.: Shaking table tests on the lateral response of a pile buried in liquefied sand, Soil Dynamic and Earthquake Engineering 26(2), 287–295 (2006).
15. Hazarika, H., Watanabe, N., Sugahara, H. and Suzuki, Y.: Influence of placement and configuration of small diameter steel pipe pile on slope reinforcement, Proceedings of the 19th International Conference on Soil Mechanics and Geotechnical Engineering, 2151-2154, ICSMGE, South Korea (2017).
16. Ma, N., Wu, H.G., Ma, H.M., Wu, X.Y. and Wang, G.H.: Examining dynamic soil pressure and the effectiveness of different pile structure inside reinforced slopes using shaking table tests, Soil Dynamics and Earthquakes Engineering 116, 293-303 (2019).
17. Qin, C.J., Hazarika, H., Pasha, S. M. K., Furuichi, H., Kochi, Y., Matsumoto, D., Fujishiro, T., Ishibashi, S., Watanabe, N. and Yamamoto, S.: Evaluation of hybrid pile supported system for protecting road embankment under seismic loading, Advances in Sustainable Construction and Resource Management, 733-744 (2021).
18. Iai, S.: Similitude for shaking table tests on soil-structure-fluid model in 1g gravitational field, Soils and Foundations 29(1), 105–118 (1989).
19. Zhang, F., Kimura, M., Nakai, T. and Hoshikawa, T.: Mechanical behavior of pile foundations subjected to cyclic lateral loading up to the ultimate state, Soils and Foundations, 40(5), 1–17 (2000).